Diffusion tensor imaging in evaluation of posterior fossa tumors in children on a 3T MRI scanner

Zarina Abdul Assis, Jitender Saini[1], Manish Ranjan[2], Arun Kumar Gupta[1], Paramveer Sabharwal[1], Purushotham R Naidu[3]

Department of Radiology, Sri Sathya Sai Institute of Higher Medical Sciences, [1]Departments of Neuroimaging and Interventional Radiology and [2]Neurosurgery, National Institute of Mental Health and Neurosciences, [3]Senior Medical Advisor, Biocon Ltd, Bangalore, Karnataka, India

Correspondence: Dr. Zarina Abdul Aziz, Department of Radiology, Sri Sathya Sai Institute of Higher Medical Sciences, EPIP Area, Whitefeild, Bangalore - 560 066, Karnataka, India. E-mail: drzarinaaziz@gmail.com

Abstract

Context: Primary intracranial tumors in children are commonly located in the posterior fossa. Conventional MRI offers limited information regarding the histopathological type of tumor which is essential for better patient management. **Aims:** The purpose of the study was to evaluate the usefulness of advanced MR imaging techniques like diffusion tensor imaging (DTI) in distinguishing the various histopathological types of posterior fossa tumors in children. **Settings and Design:** DTI was performed on a 3T MRI scanner in 34 untreated children found to have posterior fossa lesions. **Materials and Methods:** Using third party software, various DTI parameters [apparent diffusion coefficient (ADC), fractional anisotropy (FA), radial diffusivity, planar index, spherical index, and linear index] were calculated for the lesion. **Statistical Analysis Used:** Data were subjected to statistical analysis [analysis of variance (ANOVA)] using SPSS 15.0 software. **Results:** We observed significant correlation ($P < 0.01$) between ADC mean and maximum, followed by radial diffusivity (RD) with the histopathological types of the lesions. Rest of the DTI parameters did not show any significant correlation in our study. **Conclusions:** The results of our study support the hypothesis that most cellular tumors and those with greater nuclear area like medulloblastoma would have the lowest ADC values, as compared to less cellular tumors like pilocytic astrocytoma.

Key words: Apparent diffusion coefficient; children; diffusion tensor imaging; fractional anisotropy; linear index; planar index; posterior fossa tumors; radial diffusivity; spherical index

Introduction

Brain tumors are a serious and major health problem, especially in children. Brain tumors are the most common solid neoplasm in children, with incidence varying between 1 and 3 per 100,000 population.[1] Between 54% and 70% of all childhood brain tumors originate in the posterior fossa. Certain types of posterior fossa tumors, such as medulloblastoma, ependymomas, and astrocytomas of the cerebellum and brain stem, occur more frequently in children.[1]

Tumors in the posterior fossa are critical, primarily because of the limited space within the posterior fossa and the potential involvement of vital brain stem structures. It is also important to note that the tumors within posterior fossa are heterogenous and these tumors have different natural course and prognosis. In terms of surgical approach, the surgical strategy differs with different tumors and the anatomical territory involved or infiltrated. Hence, it becomes important to diagnose with fair degree of confidence regarding the nature and extent of tumor. Conventional MRI is essential for diagnosis as well as evaluation of location, size, tissue characteristics, and extent

of the tumor, but often offers limited information regarding tumor grade and type.

Diffusion tensor imaging (DTI) is a novel imaging technique that describes the 3D diffusion phenomenon of the protons as per the microenvironmental properties, providing a unique description of the space where this molecular movement takes place. DTI measures the apparent diffusion coefficient (ADC) and diffusion anisotropy of water in tissue.[2] Various studies have been reported in the past correlating the DTI parameters like ADC and fractional anisotropy (FA) with the histopathological types and grades of tumors. However, till date, there are no studies correlating other DTI parameters like radial diffusivity (RD), planar index, spherical index, and linear index with posterior fossa tumors in children.

The purpose of this study was to prove the usefulness of DTI as a diagnostic tool in categorizing common benign and high-grade posterior fossa tumors in children, which can help clinicians in prognostication as well as proper treatment planning. Also, we intent to prove the well-known hypothesis that tumor with high cellularity and higher nuclear–cytoplasmic ratio will show lower ADC and higher FA. This study, to the best of our knowledge, is the first of its kind to correlate various DTI parameters other than ADC and FA, like RD, planar index, spherical index, and linear index, with posterior fossa tumors in children.

Materials and Methods

The study was conducted at a national tertiary care center with dedicated neurological setting after obtaining ethical approval. Patients who had undergone some form of prior tumor resection or radiotherapy in the past were not included in the study. Patients under the age of 18 years were only included in the study. Those patients who could not cooperate for the scan were imaged under sedation, under strict monitoring by a neuroanesthesiologist.

Data collection
The MR imaging was performed on a 3T Philips Acheiva scanner. The MRI scans were obtained by first performing a three-plane localizer scan, followed by an axial turbo spin-echo T2-weighted scan (TR/TE 3270/80 ms, flip angle 90°, field of view (FOV) 250 mm, Acquisition (ACQ) voxel size 0.89/1.21/5.00 mm, slice thickness/gap 5 mm/1 mm) and T2-weighted fluid-attenuated inversion recovery (FLAIR) sense (TR/TE 11,000/120 ms, flip angle 90°, FOV 250 mm, ACQ voxel size 0.96/1.79/5.00 mm, slice thickness/gap 5 mm/1 mm). T1WI, Gradient recall echo (GRE), and post-contrast T1WI were also obtained.

DTI was obtained using 16 directions (DWISE, TR/TE = 8987/61.2 ms, no. of slices 70, FOV 224 mm, ACQ voxel size 2/2/2 mm, slice thickness/gap 2 mm/0 mm, no. of directions 16, B values = 0, 1000). Total scan duration including routine sequences and post-contrast imaging, along with 16-direction DTI was approximately 40 min.

Post-processing of DTI was performed by third party software named DTI Studio (DTI studio latest x86.exe- 3s bit version). All the DTI parametric maps were created, including FA, relative anisotropy (RA), volume ratio (VR), tensor trace (TT; which is calculated by multiplying the ADC by 3), linear index (cL), planar index (cP), spherical index (cS), and RD [Figure 1]. Using circular region of interest (ROI) tracer, the ROIs were manually traced [Figure 2] to include the entire tumor on axial images at three fixed levels, i.e. superior, middle, and inferior cerebellar peduncles, since all tumors were large and extended from superior to inferior cerebellar peduncles. Mean of these three values was then calculated to represent a single lesion. Henceforth, the term ADC (calculated as
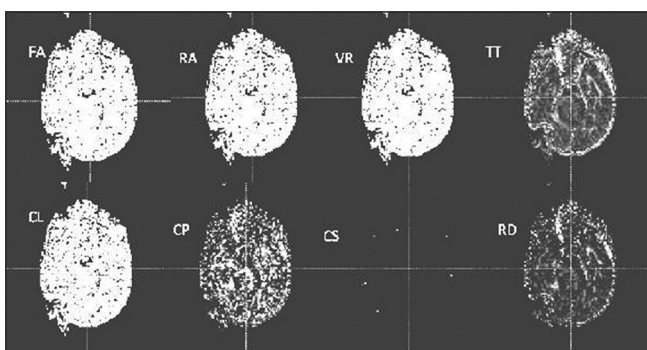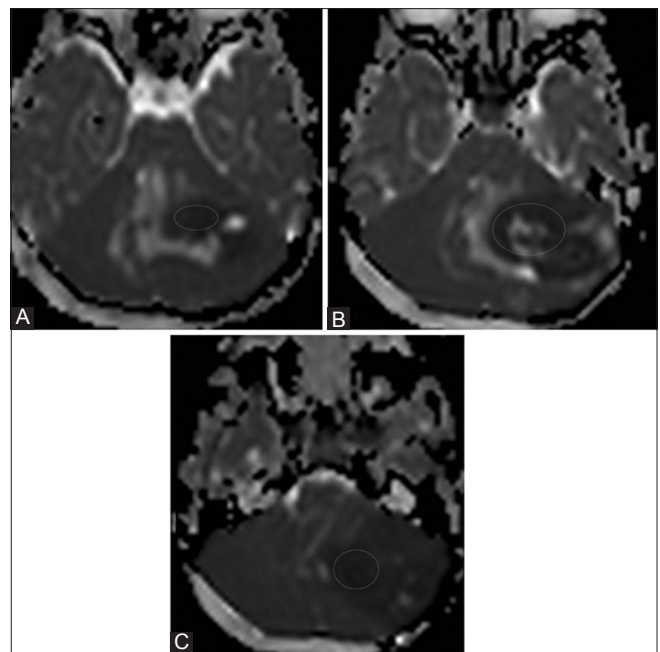

Figure 2 (A-C): ADC map in a case of medulloblastoma depicting the method used to draw circular ROIs at the level of superior (A), middle (B), and inferior (C) cerebellar peduncles

Figure 1: DTI parametric maps created for calculation of FA, RA, VR, TT, CL, CP, CS, and RD in a case of medulloblastoma

TT/3), instead of TT, will be used in this article for the purpose of easy understanding by readers.

The required sample size for this type of study was calculated as approximately 35 subjects. Data were subjected to statistical analysis [analysis of variance (ANOVA)] using SPSS 15.0 software.

Results

Patient characteristics

Thirty-four children diagnosed with posterior fossa space-occupying lesions on CT or conventional MRI, with or without ventriculoperitoneal (VP) shunting, were enrolled in the study, of which majority (23/34) were in the first decade (age range: 3-17 years; mean 10 ± 3.47) and the gender representation was similar (16 males vs. 18 females). Most of the patients (29/34) presented with features of raised intracranial pressure (ICP) followed by acute (2/34) or long-standing ataxia (3/34).

Of the posterior fossa lesions studied, most of the lesions were located in the cerebellar hemisphere (44.1%) followed by vermis (32.4%). Irrespective of the locations of the lesions, they were either in the midline (52.9%) or off-center axis (47.1%), and majority (55.9%) were less than 100 cm^3 in volume. Three-quarters of tumors (73.5%) were predominantly solid, while one-fifth of tumors (20.6%) were predominantly cystic. Six percent of tumors were mixed in nature. Majority of the lesions (82.4%) were well-circumscribed. Susceptibility artifacts suggestive of calcification/hemorrhage on conventional MRI gradient echo sequence were noted in 23.5% of tumors. Cerebrospinal fluid (CSF) seeding was noted in five cases (14.7%) at the time of diagnostic MRI study.

On histopathological examination, the most common lesion diagnosed was pilocytic astrocytoma (14/34), followed by medulloblastoma (8/34). The details of the histopathological diagnosis and demographics are presented in Table 1.
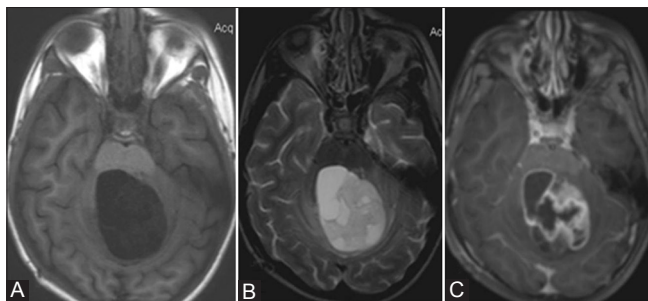
Pilocytic astrocytoma (WHO Grade 1) presented as a solid lesion with macrocysts in 7/14 patients, cysts with mural nodule in 4/14 patients, and mixed form in the rest (3/14). Almost all the cases of pilocytic astrocytoma showed hypointensity on T1WI and hyperintensity on T2WI, with heterogeneous enhancement [Figure 3].

All the cases of medulloblastoma (WHO Grade 4) presented as predominantly solid tumors with either microcystic or macrocystic changes, with majority showing iso- to hypointensity on both T1WI and T2WI with heterogeneous contrast enhancement [Figure 4].

Children with anaplastic ependymoma (WHO Grade 3) presented with solid heterogeneous mixed intensity lesions [Figure 5]. Hemangioblastomas presented as typical peripherally located cystic lesion with intensely enhancing mural nodule. Another case who presented as a cerebellar cyst with mural nodule was diagnosed as cerebellar ganglioglioma [Figure 6]. Atypical teratoid rhabdoid tumor (ATRT) was diagnosed in a 4-year-old female, which appeared as a predominantly solid lesion with T1 isointensity and T2 hypointensity and with homogeneous enhancement [Figure 7]. Two older females presented with acute raised ICP features with

Table 1: Distribution of the various histopathological diagnoses among the 34 patients

Histopath diagnosis	WHO grading of tumor	Number of patients *n* (%)
Medulloblastoma	Grade IV	8 (23.5)
Pilocytic astrocytoma	Grade I	14 (41.2)
Anaplastic ependymoma	Grade III	3 (8.8)
Atypical teratoid rhabdoid tumor	Grade IV	1 (2.9)
Choroid plexus papilloma	Grade I	1 (2.9)
Exophytic brainstem glioma	Grade II	1 (2.9)
Hemangioblastoma	Grade I	2 (5.8)
Brainstem glioblastoma	Grade IV	1 (2.9)
Cerebellar ganglioglioma	Grade I	1 (2.9)
Infectious cerebellitis	-	2 (5.8)

WHO: World Health Organization

Figure 3 (A-C): A 7-year-old female with pilocytic astrocytoma. (A) Axial T1 W image showing well-defined hypointense cystic lesion with solid components (B) Axial T2W image showing hyperintense lesion with heterogenous solid components and mild perilesional edema (C) Axial T1W post-contrast image showing heterogeneous enhancement of the lesion
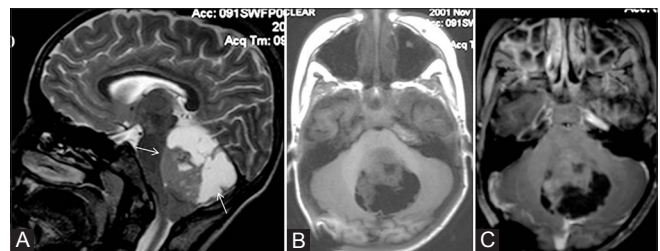

Figure 4 (A-C): A 5-year-old boy with classical medulloblastoma. (A) Sagittal T2W image showing mixed solid–cystic midline lesion (white arrows), with the solid component isointense on T2 (B) Axial T1W image showing T1-isointense solid component and T1-hypointense cystic areas (C) Axial T1W post-contrast image showing minimal enhancement of the solid component

conventional imaging showing focal ill-defined bulky lesions in the cerebellar hemispheres, but they showed complete resolution following treatment with steroids/ anti-tuberculosis treatment (ATT), and hence were categorized as inflammatory cerebellitis [Figures 8 and 9]. Another 10-year-old boy who presented with a focal sharply marginated T2-hyperintense and T1-hypointense brainstem mass with moderate peripheral enhancement and delayed centripetal filling in of the contrast was found to have brainstem glioblastoma (WHO Grade 4) [Figure 10].

DTI analysis

On analysis of the various DTI parameters, the most significant parameters strongly correlating with the tumor histopathology were maximum and mean ADC values (with a $P < 0.01$ each), maximum cP value ($P < 0.01$),

and minimum RD value ($P < 0.01$) [Table 2]. The other statistically significant parameters were minimum TT and maximum and mean RD values [Table 2]. The parameter with the most significant correlation with the histopathology of tumors was mean ADC ($P = 0.003$). The mean value of ADC was 0.9×10^{-3} for medulloblastomas, 1.7×10^{-3} for pilocytic astrocytomas, and 1.06×10^{-3} for anaplastic ependymomas. FA values did not show any significant trend in classifying the lesions. A comparison between the major tumor types (pilocytic astrocytoma, medulloblastoma, and anaplastic ependymoma) showed a significant correlation of ADC mean in differentiating between pilocytic astrocytoma and medulloblastoma ($P = 0.002$), followed by RD minimum ($P = 0.005$). Details of the rest of the parameters and their correlation with histopathological diagnosis are also elaborated in Table 2.
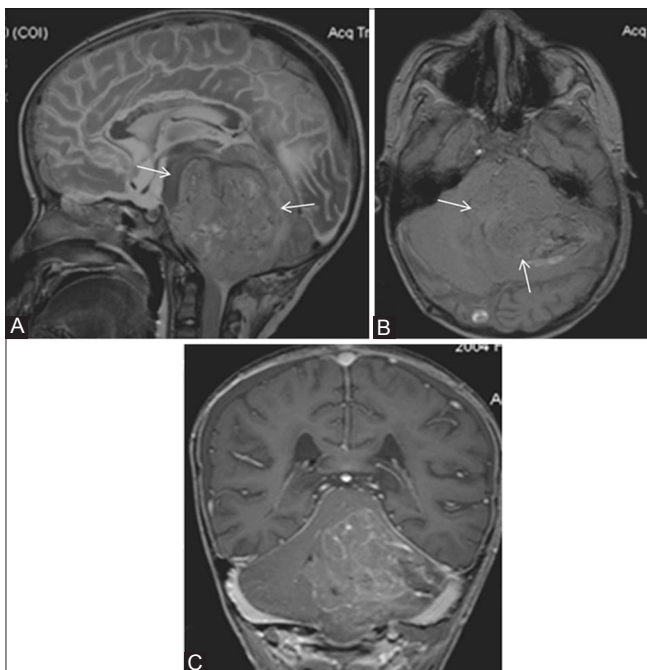

Figure 5 (A-C): A 6-year-old boy with anaplastic ependymoma. (A) Sagittal T2W image showing large heterointense predominantly solid lesion (white arrows) (B) Axial T1 W image showing predominantly isointense lesion with patchy areas of hyperintensities, with off-midline location (C) Coronal T1W post-contrast image showing moderate heterogeneous enhancement of the lesion
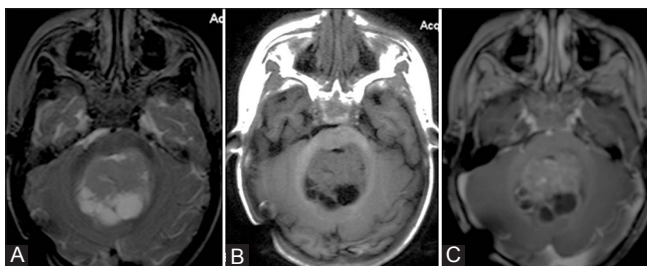

Figure 6 (A-C): An 11-year-old female with cerebellar ganglioglioma. (A) Sagittal T2W image showing fairly well-defined mixed solid cystic lesion (B) Axial T2 FLAIR image showing no inversion of cystic contents (C) Axial T1W post-contrast image showing homogeneous enhancement of the solid component and cystic wall enhancement

Figure 7 (A-C): A 4-year-old female with atypical teratoid rhabdoid tumor. (A) Axial T2 W image showing mixed solid–cystic lesion in midline (B) Axial T1W image showing isointense solid component (C) Axial T1W post-contrast image showing moderate enhancement of the solid component
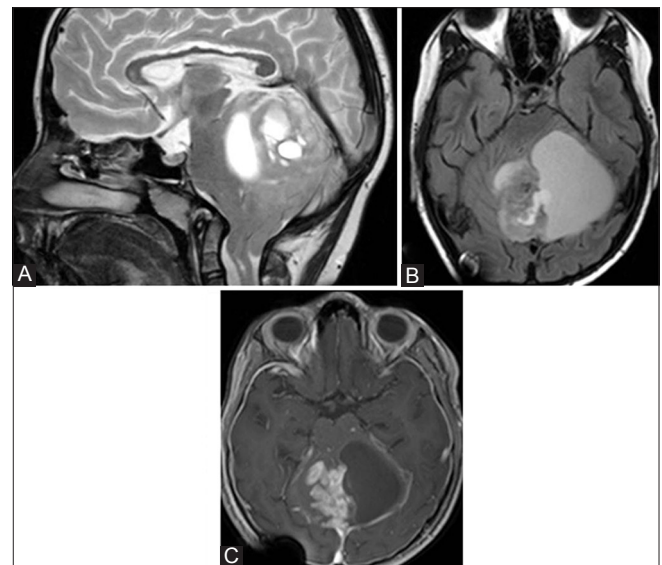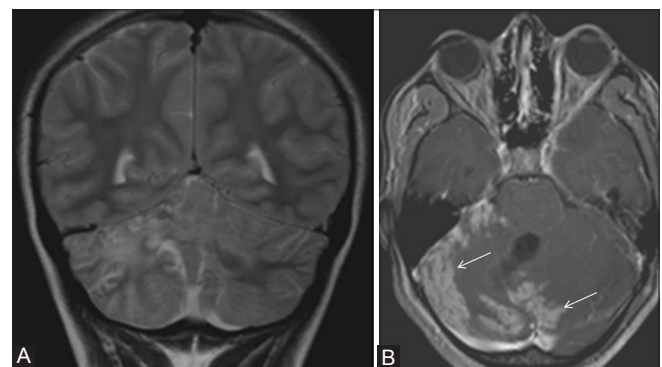

Figure 8 (A and B): A 14-year-old female with tubercular cerebellitis. (A) Coronal T2W image showing patchy cerebellar edema with few foci of T2 hypointensities (B) Axial T1W post-contrast image showing patchy folial pattern of thick enhancement (white arrows)
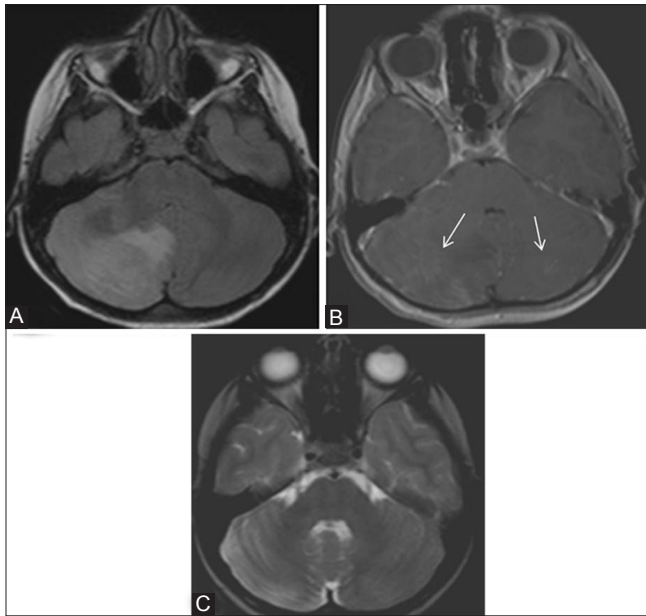
Figure 9 (A-C): A 16-year-old female with viral cerebellitis. (A) Axial T2W FLAIR image showing diffuse bilateral cerebellar edema (right side more than left side) (B) Axial T1W post-contrast image showing subtle patchy enhancement (C) 3 months follow-up axial T2W image showing complete resolution of the edema and mass effect

Discussion

Pediatric brain tumors are heterogeneous in nature and are one of the most challenging clinical scenarios not only to the practicing neurosurgeon but also to neuroradiologists. Preoperative surgical planning depends upon a careful review of neuroimaging. Current conventional diagnostic MR imaging techniques provide limited information regarding tumor type and grade.[3]

Diffusion imaging is a relatively old technique which produces images related to microscopic displacement of water molecules. DTI is a newer and more sophisticated quantitative form of diffusion imaging. With DTI, it is possible to calculate not only an absolute measure of average water diffusion for each voxel (the ADC) but also how water diffusion varies along different axes of the image (diffusion anisotropy). Overall, both ADC and diffusion anisotropy reflect the microstructure of the tissue in which they are measured.[4]

ADC values cannot be generalized for differentiating brain tumor types and grades, even though there is an established negative correlation with glioma grades. ADC also does not seem helpful in distinguishing tumor tissue from peritumoral edema.[5] On the other hand, the ADC has been reported reliable for characterizing some pediatric brain tumors.[6] ADC also has therapeutic implications, as pre-treatment diffusion values predict tumor response to radiation therapy[7] and are valuable
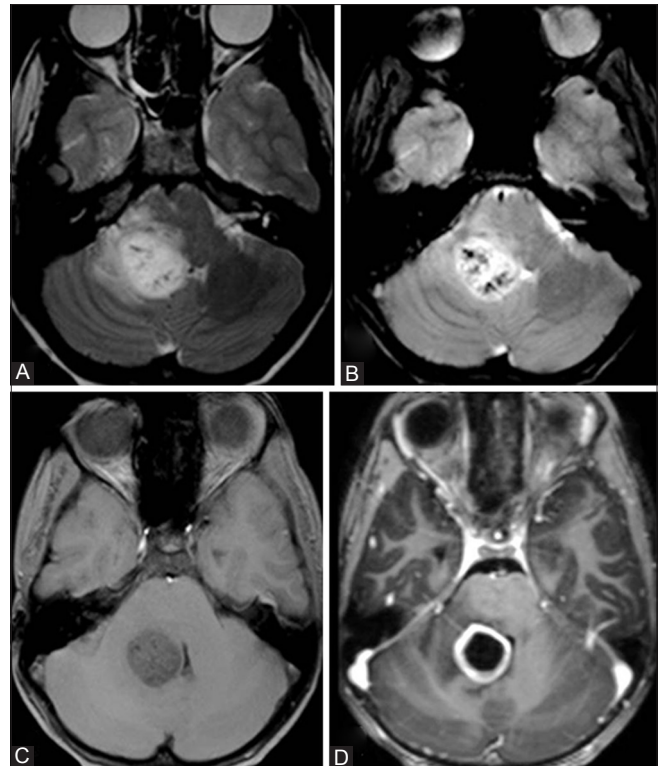

Figure 10 (A-D): A 12-year-old male with glioblastoma multiforme (GBM) (A) Axial T2W image showing hyperintense right middle cerebellar peduncle lesion with perilesional edema (B) Axial T2W GRE image showing multiple foci of blooming within the lesion (C) Axial T1W image showing the lesion to be slightly hypointense (D) Axial T1W post-contrast image showing thick rim enhancement of the lesion

in differentiating radiation-induced brain injury from tumor recurrence.

A study by Guo *et al.*[8] in 2002 using an ROI-based approach addressed the correlation between ADC and cellularity in lymphomas and high-grade astrocytomas. They demonstrated the ADC ratios were significantly higher in astrocytomas than lymphomas and suggested that ADC values reflect the tumor cellularity. Another study conducted in 2001 found that minimal tumor ADC (the least ADC value recorded in the solid part of tumor) correlated with the tumor grade, in which lower ADC values were noted in high-grade gliomas in comparison to low-grade gliomas.[9] Beppu *et al.* reported the correlation between the FA and cell density and proliferation in astrocytomas, with higher FA values corresponding to higher cell densities.[10]

Price *et al.*[11] used a different method of analysis that splits the diffusion tensor into pure isotropic and anisotropic components, and reported that DTI is 98% sensitive and 81% specific in identify tumor infiltration.

In pediatric brain tumors, it is also observed that a correlation exists between the ADC and both the tumor

Table 2: Correlation of FA, RA, VR, TT (3×ADC), cL, cP, cS, and RD with histopathological diagnosis

Variables	Histopathological diagnosis				P value
	Medulloblastoma (n=8)	Pilocytic astrocytoma (n=14)	Anaplastic ependymoma (n=3)	Others (n=9)	
FA					
Max	0.5450±0.1077	0.4714±0.1225	0.5733±0.0306	0.4511±0.0914	0.162
Min	0.0263±0.0052	0.0279±0.008	0.0233±0.0058	0.0278±0.0097	0.805
Mean	0.1663±0.0151	0.1436±0.0363	0.1367±0.0058	0.1378±0.0447	0.322
RA					
Max	0.5175±0.1514	0.4347±0.1229	0.59±0.0265	0.41±0.1084	0.087[+]
Min	0.0200±0.000	0.0231±0.0077	0.02000±0.000	0.0200±0.0087	0.627
Mean	0.1363±0.0151	0.1171±0.0300	0.1133±0.0058	0.1156±0.0371	0.393
VR					
Max	0.4038±0.2034	0.2926±0.1469	0.4667±0.0577	0.2319±0.1595	0.072[+]
Min	0.0007±0.0001	0.0015±0.0018	0.0006±0.0001	0.0015±0.0019	0.511
Mean	0.0375±0.0104	0.029±0.0137	0.03±0.000	0.0282±0.0181	0.501
TT (3×ADC)					
Max	0.0078±0.0012	0.0085±0.0015	0.0058±0.0005	0.0066±0.0017	0.008**
Min	0.0011±0.0003	0.0025±0.001	0.0018±0.0005	0.003±0.0023	0.032*
Mean	0.0027±0.0002	0.0052±0.0018	0.0032±0.0006	0.0041±0.0015	0.003**
cL					
Max	0.5013±0.0781	0.4336±0.0995	0.5133±0.0115	0.3956±0.0834	0.058[+]
Min	0.0083±0.0018	0.0104±0.0093	0.0077±0.0012	0.0072±0.002	0.661
Mean	0.1513±0.0155	0.1264±0.0265	0.13±0	0.1256±0.0364	0.175
cP					
Max	0.485±0.0393	0.3807±0.0759	0.4967±0.0924	0.3783±0.0933	0.006**
Min	0.0061±0.0015	0.0055±0.0025	0.0053±0.0015	0.0071±0.0025	0.415
Mean	0.1225±0.0104	0.1079±0.0249	0.1100±0.000	0.1078±0.0259	0.448
cS					
Max	0.9525±0.0071	0.9486±0.0146	0.9567±0.0058	0.95±0.0158	0.764
Min	0.2888±0.1158	0.3436±0.1161	0.2833±0.0289	0.400±0.0906	0.154
Mean	0.7238±0.0226	0.7636±0.0492	0.7533±0.0058	0.7756±0.0688	0.183
RD					
Max	0.0025±0.0004	0.0026±0.0005	0.0017±0.0002	0.0021±0.0006	0.013*
Min	0.0003±0.000	0.0007±0.0003	0.0005±0.0001	0.0006±0.0002	0.005**
Mean	0.0008±0.0001	0.0016±0.0006	0.0009±0.0003	0.0011±0.0007	0.016*

FA: Fractional anisotropy, RA: Relative anisotropy, VR: Volume ratio, TT: Tensor trace=3×ADC, cL: Linear index, cP: Planar index, cS: Spherical index, RD: Radial diffusivity [+]Suggestive significance (P value: $0.05 < P < 0.10$), *Moderately significant (P value: $0.01 < P \leq 0.05$), **Strongly significant (P value: $P \leq 0.01$)

grading and cellularity. It was shown that ADC value is a useful tool in classifying pediatric tumors.[4]

In the current study, we found that the ADC values were strongly correlating with the tumor type. Maximum and mean ADC values were the most significant factor in histopathological correlation of the tumor. Medulloblastoma showed statistically significant lower ADC values (maximum and mean) as compared to both pilocytic astrocytomas and anaplastic ependymomas. RD minimum (RD-min) value was also found to be significant in our study, which showed the least value in medulloblastoma, followed by anaplastic ependymomas, and the greatest value in pilocytic astrocytoma. Medulloblastoma is a highly cellular tumor with compactly arranged cells and high nuclear-cytoplasmic ratio, resulting in decreased diffusivity of the proton

molecules in the tumor microstructure,[12] while pilocytic astrocytoma has a biphasic pattern of astrocytes placed in a loose gliofibrillary stroma giving ample space for the proton molecules to diffuse randomly, possibly contributing to the difference in the ADC values.[13]

We could not find any statistically significant observation in other pathologies, as these lesions were lesser in number. The two cases of inflammatory cerebellitis were included in the study as they presented as space-occupying lesions on MRI and were difficult to differentiate from neoplasm. However, conventional MRI features like diffuse cerebellar involvement with ill-defined margins, involvement of the cerebellar gray matter, and associated leptomeningeal enhancement can help in differentiating cerebellitis (either inflammatory or demyelinating) from

neoplasms.[14] Also, a close follow-up MR imaging may show complete resolution of the lesions, sometimes healing with residual cerebellar atrophy.[14] On DTI analysis, inflammatory cerebellitis showed a trend toward relatively low RA maximum (RA-max), VR maximum (VR-max), cP maximum (cP-max), and RD mean (RD-mean). These values suggest that there could be relative restriction in the movement of the proton molecules in infection/inflammation due to the presence of extensive interstitial edema and numerous inflammatory cells like neutrophils and macrophages.

In our study, the ADC values clearly correlated with the histopathological diagnosis between two major diagnoses of pediatric brain tumors in posterior fossa. Medulloblastoma and pilocytic astrocytoma can be diagnosed preoperatively, if ADC values are considered in routine diagnostic study. An ADC value of less than 0.9×10^{-3} mm²/s suggests diagnosis of medulloblastoma, while an ADC value more than 1.3×10^{-3} mm²/s suggests diagnosis of pilocytic astrocytoma. Our study further supports the result reported by Rumboldt *et al*. in 2006, who suggested that the ADC values are 100% specific in differentiating medulloblastoma and juvenile pilocytic astrocytoma (JPA).[15] The authors also proposed ADC cutoff values of $>1.4 \times 10^{-3}$ mm²/s for JPA and $<0.9 \times 10^{-3}$ mm²/s for medulloblastoma.

In a recent study in 2010,[16] medulloblastoma and JPA were differentiated by DWI alone in 88% cases. Ependymoma could not be reliably differentiated from medulloblastoma or JPA, as in our study.

Also, in the current study, FA had no diagnostic value in differentiating between various posterior fossa lesions. Beppu *et al*. demonstrated a linear increase in FA and cell density in case of gliomas.[8] However, other studies showed decrease in FA with increased cell density. In 2006, Stadlbauer *et al*. proposed that as normal white matter shows high FA values due to the neural fibers, it is reasonable that areas with less tumor infiltration will show a higher FA.[17]

Only a few studies have focused on other DTI parameters like cL, cP, cS, and RD in tumors. In 2009, Jolapara *et al*. studied these parameters in epidermoid cysts and correlated the findings with the histopathological findings.[18] Another study by Jolapara *et al*. in 2011 was on the role of FA and spherical anisotropy in preoperative grading of diffusely infiltrating astrocytomas.[19] There are no studies to date correlating these novel DTI parameters in posterior fossa tumors in children, to the best of our knowledge.

The results support our hypothesis that the most cellular tumors and those with the least amount of cytoplasm (greater nuclear area) would have the lowest ADC values. The present study also proves that quantitative DTI improves the MR imaging of pediatric CNS malignancies *in vivo*. Though our sample size was relatively small and we did not study the direct correlation of histopathological parameters like nuclear-cytoplasmic ratio, tumor cell density, or microvascular proliferation index of these lesions, this information could play an important adjunctive role in the workup and treatment of pediatric CNS neoplasms.

Conclusion

The ADC values reflect the tumor cellularity and possible nature of the tumor. The ADC values are lower for most cellular tumors and tumors with greater nuclear area like medulloblastoma, while they are higher in tumors with less cellularity like pilocytic astrocytoma. Quantitative DTI study reasonably differentiates between the common types of posterior fossa tumors in children. These findings could be a value addition in the diagnosis and treatment of pediatric CNS neoplasms.

References

1. Poretti A, Meoded A, Huisman TA. Neuroimaging of pediatric posterior fossa tumors including review of the literature. J Magn Reson Imaging 2012;35:32-47.

2. Bahn MM. Invariant and orthonormal scalar measures derived from magnetic resonance diffusion tensor imaging. J Magn Reson 1999;141:68-77.

3. Chen X, Weigel D, Ganslandt O, Buchfelder M, Nimsky C. Diffusion tensor imaging and white matter tractography in patients with brainstem lesions. Acta Neurochir (Wien) 2007;149:1117-31.

4. Gauvain KM, McKinstry RC, Mukherjee P, Perry A, Neil JJ, Kaufman BA, *et al*. Evaluating pediatric brain tumor cellularity diffusion-tensor imaging. AJR Am J Roentgenol 2001;177:449-54.

5. Pauleit D, Langen KJ, Floeth F, Hautzel H, Riemenschneider MJ, Reifenberger G, *et al*. Can the apparent diffusion coefficient be used as a noninvasive parameter to distinguish tumor tissue from peritumoral tissue in cerebral gliomas? J Magn Reson Imaging 2004;20:758-64.

6. Tzika AA, Zarifi MK, Goumnerova L, Astrakas LG, Zurakowski D, Young-Poussaint T, *et al*. Neuroimaging in pediatric brain tumors: Gd-DTPA-enhanced, hemodynamic, and diffusion MR imaging compared with MR spectroscopic imaging. AJNR Am J Neuroradiol 2002;23:322-33.

7. Mardor Y, Roth Y, Ochershvilli A, Spiegelmann R, Tichler T, Daniels D, *et al*. Pretreatment prediction of brain tumors' response to radiation therapy using high b-value diffusion-weighted MRI. Neoplasia 2004;6:136-42.

8. Guo AC, Cummings TJ, Dash RC, Provenzale JM. Lymphomas and high-grade astrocytomas: Comparison of water diffusibility and histologic characteristics. Radiology 2002;224:177-83.

9. Kono K, Inoue Y, Nakayama K, Shakudo M, Morino M, Ohata K, *et al*. The role of diffusion-weighted imaging in patients with brain tumors. AJNR Am J Neuroradiol 2001;22:1081-8.

10. Beppu T, Inoue T, Shibata Y, Yamada N, Kurose A, Ogasawara K, *et al*. Fractional anisotropy value by diffusion tensor magnetic resonance imaging as a predictor of cell density and proliferation activity of glioblastomas. Surg Neurol 2005;63:56-61.

11. Price SJ, Burnet NG, Donovan T, Green HA, Peña A, Antoun NM,

et al. Diffusion tensor imaging of brain tumours at 3T: A potential tool for assessing white matter tract invasion? Clin Radiol 2003;58:455-62.

12. Ellison D. Classifying the medulloblastoma: Insights from morphological and molecular genetics. Neuropathol Appl Neurobiol 2002;28:257-82.

13. Kleihues P, Louis DN, Scheithauer BW, Rorke LB, Reifenberger G, Burger PC, *et al*. The WHO classification of tumours of the nervous system. J Neuropathol Exp Neurol 2002;61:215-29.

14. Tlili-Graiess K, Mhiri Souei M, Mlaiki B, Arifa N, Moulahi H, Jemni Gharbi H, *et al*. Imaging of acute cerebellitis in children. Report of 4 cases. J Neuroradiol 2006;33:38-44.

15. Rumboldt Z, Camacho DL, Lake D, Welsh CT, Castillo M. Apparent diffusion coefficients for differentiation of cerebellar tumors in children. AJNR Am J Neuroradiol 2006;27:1362-9.

16. Jaremko JL, Jans LB, Coleman LT, Ditchfield MR. Value and limitations of diffusion-weighted imaging in grading and diagnosis of pediatric posterior fossa tumors. AJNR Am J Neuroradiol 2010;31:1613-6.

17. Stadlbauer A, Ganslandt O, Buslei R, Hammen T, Gruber S, Moser E, *et al*. Gliomas: Histopathologic evaluation of changes in directionality and magnitude of water diffusion at diffusion-tensor MR imaging. Radiology 2006;240:803-10.

18. Jolapara M, Kesavadas C, Radhakrishnan VV, Saini J, Patro SN, Gupta AK, *et al*. Diffusion tensor mode in imaging of intracranial epidermoid cysts: One step ahead of fractional anisotropy. Neuroradiology 2009;51:123-9.

19. Jolapara M, Patro SN, Kesavadas C, Saini J, Thomas B, Gupta AK, *et al*. Can diffusion tensor metrics help in preoperative grading of diffusely infiltrating astrocytomas? A retrospective study of 36 cases. Neuroradiology 2011;53:63-8.